



Tracer Shape and Local Media Structure Determine the Trend of Translation-Rotation Decoupling in Two-Dimensional Colloids

Jeongmin Kim and Bong June Sung*

*Department of Chemistry and Research Institute for Basic Science, Sogang University,
Seoul 121-742, Republic of Korea*

(Received 18 May 2015; published 7 October 2015)

The translational diffusion of tracers in glass-forming materials often violates the Stokes-Einstein relation while their rotation follows the Debye-Stokes-Einstein relation faithfully, thus decoupling translational and rotational diffusion. In this Letter, we show by performing molecular dynamics simulations for two-dimensional (2D) colloids that the tracer shape and the local media structure are critical such that rotational diffusion is either suppressed or enhanced depending on the tracer shape. For square tracers dissimilar in structure to the local media structure of 2D colloids, the translation-rotation decoupling occurs and the rotational diffusion is enhanced relative to the translation. For sufficiently large diamond tracers similar in structure to the local media structure, tracers undergo rotational hopping motions and their rotation is suppressed relative to the translation. For distorted-diamond tracers, the decoupling is marginal. Translational diffusion does not change significantly with the tracer shape and obeys the Stokes-Einstein relation.

DOI: [10.1103/PhysRevLett.115.158302](https://doi.org/10.1103/PhysRevLett.115.158302)

PACS numbers: 82.70.Dd, 61.20.Lc, 64.70.pm, 64.70.pv

Translational (D_T) and rotational (D_R) diffusion coefficients of tracers in various complex systems often decouple from each other [1–10] even though Stokes-Einstein (SE) and Debye-Stokes-Einstein (DSE) relations suggest that D_T/D_R should be constant over a range of temperature. It is called the translation-rotation decoupling, one of the hallmarks of glassy dynamics. How the translation-rotation decoupling occurs and how the decoupling would relate to the local media structure still remain elusive. It is partly because the values of D_R estimated via the Debye formalism (using rotational relaxation time) and Einstein formalism (using mean-square angular displacement) are different in some systems [5–7]. The shape, size, and interparticle interactions of tracers were different in different studies, which also makes systematic investigation challenging [9–15]. In this work, we compare tracers of different shape but similar size and interparticle interactions in two-dimensional (2D) colloidal suspensions. We show that the choice of the tracer shape could be critical, such that the translation-rotation decoupling occurs in qualitatively different fashions depending on tracer shape. Considering that the tracers are stand-ins to interrogate the 2D colloid dynamics, the effects of the tracer shape indicate that the local media structure should relate to the dynamic heterogeneity (DH) of 2D colloids.

The translation-rotation decoupling in glasses and supercooled liquids has been attributed to the breakdown of the SE relation and spatially heterogeneous translational diffusion, i.e., the presence of domains of different mobility [1–3,16,17]. D_R , on the other hand, remains faithful to the DSE relation [1]. When translation and rotation decouple, translational diffusion is usually enhanced relative to

rotational diffusion [1,8,18]. A few simulation studies reported an opposite trend where rotation was enhanced relative to translation, which was, however, attributed to the discrepancy between Einstein and Debye formalisms [5–7]. Edmond *et al.* illustrated recently that when Debye and Einstein formalisms provided identical values of D_R , the translation-rotation decoupling accompanied the enhancement of translation compared to rotation [8]. In this work, we illustrate that the translation of *diamond* tracers in 2D colloid suspensions is enhanced compared to rotation while the rotation of *square* tracers is enhanced compared to translation. In the meantime, the decoupling of *distorted-diamond* tracers is marginal. Debye and Einstein formalisms provide identical D_R 's for all three types of tracers when the first-order rotational time correlation function is employed.

2D colloidal liquids have been investigated extensively because structural information such as a medium-range crystalline order may be readily accessible unlike three dimensional (3D) systems [19–26]. Monodisperse 2D colloidal suspensions also exhibit a rich phase behavior with an intermediate *hexatic* phase between isotropic liquid and solid phases [27,28]. They become dynamically heterogeneous in the hexatic and solid phases [20,23]. In 2D hexatic and solid phases with hexatic bond orientational order (HBOO), the locally favorable structure (LFS) is, of course, hexagonal, which is identical to the globally stable structure. When the tracer shape is similar to the hexagonal structure like diamond tracers, the rotation of the tracers should be affected significantly by 2D colloids. Diamond tracers undergo rotational hopping motions by integer multiples of $\pi/3$. On the other hand, square tracers,

dissimilar in structure to the local media structure, do Brownian rotational diffusion.

2D colloids are modeled as discs of diameter σ and mass m . Colloids interact with each other via a truncated and shifted Lennard-Jones potential ($U^{\text{LJ}}(r) = 4\epsilon[(r/\sigma)^{12} - (r/\sigma)^6] - U_c$, where $U_c = 4\epsilon[(r_c/\sigma)^{12} - (r_c/\sigma)^6]$ and $r_c = 2.5\sigma$). m , σ , and $k_B T$ are units of mass, length, and energy in this study, respectively, where k_B denotes the Boltzmann constant. The time unit is $\tau = \sqrt{m\sigma^2/k_B T} = 1$. All three different shapes of tracers are composed of 16 discs of diameter σ and mass m [Fig. 1(a)]. The interaction between discs of tracers is described by the Weeks-Chandler-Andersen potential to prevent the aggregation of tracers. The interaction between the discs of tracers and colloids is described via U^{LJ} .

Intraparticle interactions between discs in a single tracer are described by both harmonic bonding (U^b) and bending (U^a) potentials. All pairs of neighbor discs are bonded tightly by invoking $U^b = 100k_B T(r/\sigma - 1.2)^2$, where r is the distance between a pair of neighbor discs. There are a total of 36 bonding angles between neighbor discs for a tracer. The bending potential $U^a = 100k_B T(\theta - \theta_e)^2/\text{deg}^2$ is applied to each of the bonding angles, where θ and θ_e denote the bonding angle and its value at a potential energy minimum, respectively. The values of θ_e for 36 bonding angles are either α or $\beta = \pi - \alpha$. We tune the tracer shape by selecting the values of α and β : $(\alpha, \beta) = (60^\circ, 120^\circ)$, $(90^\circ, 90^\circ)$, and $(75^\circ, 105^\circ)$ for diamond, square, and distorted-diamond tracers, respectively [Fig. 1(a)]. The force constants for U^b and U^a are so large that tracers are effectively rigid.

Initial configurations are prepared by inserting 5 tracers and 14 296 colloids at random positions in a simulation cell

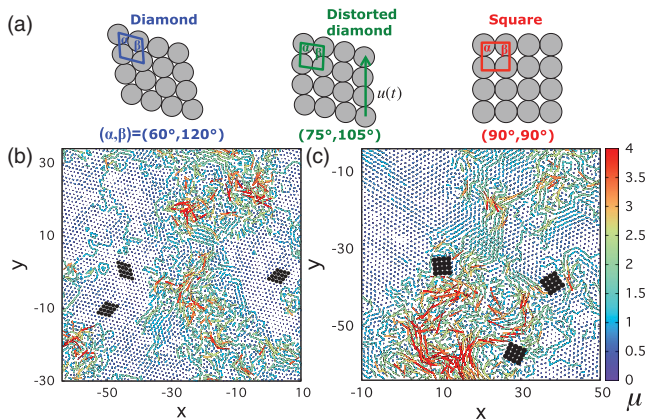


FIG. 1 (color). (a) Three types of tracers are employed: diamond, distorted diamond, and square. The values of α and β are different for different shapes. The vector $\vec{u}(t)$ is the unit vector parallel to the side of each tracer at time t . Mobility maps at $T = 0.9$ for (b) diamond tracers (black) and (c) square tracers (black) in colloids. The color code of colloids is determined based on the mobility (μ) of each colloid.

of dimension $L = 128\sigma$. Periodic boundary conditions are applied in all directions. The number density ρ in this study is about 0.88. We propagate systems in a canonical ensemble by employing the LAMMPS molecular dynamics simulator with a velocity-type Verlet integrator and Nosé-Hoover thermostat [29]. We change T from 2 to 0.8 to investigate the liquid-to-hexatic phase transition of 2D colloids. We observe and confirm the liquid-to-hexatic phase transition near $T = 1$ by calculating bond order correlation function, its susceptibility, and radial distribution function [20,23,30].

In the hexatic phase with quasi-long-range HBOO, the dynamics of 2D colloids becomes spatially heterogeneous [23]. Figures 1(b) and 1(c) depict the mobility maps of 2D colloids at $T = 0.9$ with diamond and square tracers, respectively. The mobility (μ) of each colloid is defined as a displacement of the colloid within $t = 50$, which is about the relaxation time of 2D colloids. The non-Gaussian parameter of 2D colloids is maximum at $t \approx 50$ at $T = 0.9$. The color code of 2D colloids in Fig. 1 is determined based on μ of each colloid: red colloids are mobile whereas purple colloids are sedentary. The domains of different μ are observed clearly, showing that 2D colloid dynamics in the hexatic phase is spatially heterogeneous. Recent studies showed that the surface roughness of tracers influenced the mobility of supercooled liquids: rough and smooth surfaces decreased and increased μ of the supercooled liquids, respectively [12,31]. In 2D colloids, on the other hand, the presence and the shape of tracers do not affect significantly both the mean-square displacements and the non-Gaussian parameters of 2D colloids [30].

Square tracers are more likely to be surrounded by mobile colloids while diamond tracers are surrounded mostly by sedentary colloids of $\mu \leq 1$. Figure 2(a) depicts the mobility distribution functions $P(\mu)$ of colloids around tracers. We count only colloids whose distance to the center of mass of a tracer is less than 5σ . $P(\mu)$'s are different for different shapes of tracers.

Such differences in $P(\mu)$ are attributed to how much the tracer shape is similar to HBOO of 2D colloids. We calculate the distribution function $P(|\psi_6|)$ [27] to evaluate

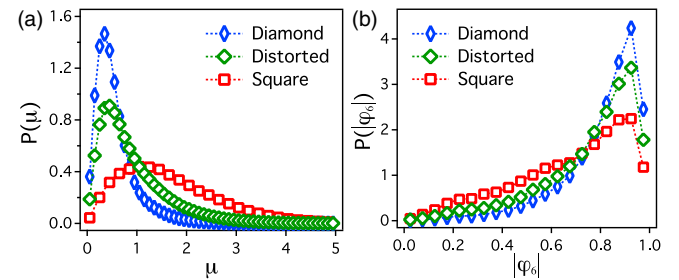


FIG. 2 (color online). Distribution functions of (a) the mobility (μ) and (b) the local orientational order ($|\psi_6|$) of colloids around tracers.

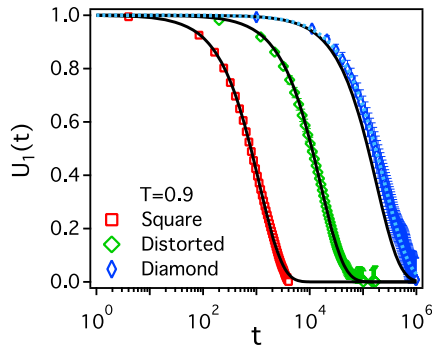


FIG. 3 (color online). Rotational time correlation functions $[U_1(t)]$ at $T = 0.9$. Solid lines are plotted by using the relation $U_1(t) = \exp(-D_R t)$ and D_R from Einstein formalism.

the local structure of colloids around tracers, where $\psi_6 \equiv (1/N_n) \sum_{j=1}^{N_n} \exp(-i6\theta_{nj})$, N_n is the number of the neighbor colloids around a particular n th colloid, and θ_{nj} denotes the angle between an arbitrary reference vector and a bond of the n th colloid and the j th neighbor colloid. $|\psi_6| = 1$ if the colloid at the center and its neighbors are arranged in a perfect hexagonal structure. As shown in Fig. 2(b), colloids around a diamond tracer are more likely to form a hexagonal structure while the hexagonal arrangement of colloids disappear the most significantly for square tracers. In other words, around square tracers there are the most defects, which may facilitate the rotational motion of square tracers.

We estimate D_T of tracers by using the mean-square displacement $\langle [\Delta r(t)]^2 \rangle (= \langle |\vec{r}(t) - \vec{r}(0)|^2 \rangle)$ and the Einstein relation. $\langle \dots \rangle$ denotes an ensemble average and $\vec{r}(t)$ is the position vector of the center of mass of a tracer at time t . There are two formalisms in order to estimate D_R : Einstein and Debye formalisms. In the Einstein formalism, we calculate the mean square angular displacement $\langle [\Delta \varphi(t)]^2 \rangle = \langle |\varphi(t) - \varphi(0)|^2 \rangle$, where $\varphi(t)$ is the unbounded angle of the vector $\vec{u}(t)$ of a tracer at time t . The vector $\vec{u}(t)$ is the unit vector parallel to the side of each tracer [Fig. 1(a)]. And D_R is obtained by using the

relation $D_R = \lim_{t \rightarrow \infty} \langle [\Delta \varphi(t)]^2 \rangle / 2t$. On the other hand, in the Debye formalism, the rotational correlation function $U_l(t)$ of tracers is considered, i.e., $U_l(t) = \langle \exp[i l \Delta \varphi(t)] \rangle$, where an integer l is the order of the rotational correlation function [15]. According to the Debye approximation, $U_{l=1}(t)$ decays exponentially, i.e., $U_1(t) = \exp(-D_R t)$. For all types of tracers used in this study, both Einstein and Debye formalisms are consistent with each other. In Fig. 3, symbols are simulation results for $U_1(t)$'s at $T = 0.9$. We plot $\exp(-D_R t)$ (solid lines) with values of D_R obtained from the Einstein formalism and find that Einstein and Debye formalisms match well with each other, indicating that the values of D_R are not affected by the formalism employed. Higher-order correlation functions $U_l(t)$ with $l \geq 2$ should also decay exponentially according to the Debye formalism. However, they become stretched near the liquid-hexatic phase transition [30]. D_R 's for square tracers obtained from $U_l(t)$ with $l \geq 2$ are hardly affected by l . On the other hand, for diamonds and distorted diamonds, D_R obtained from $U_l(t)$ decreases with an increase in l . But the trends of translation-rotation decoupling do not change (Fig. S7 in the Supplemental Material [30]).

The translational and rotational diffusion of tracers couple with each other at high temperature ($T \geq 1.5$) in 2D colloidal suspensions with D_T/D_R constant [8]. D_T and D_R of the tracers, however, decouple at low temperature near the liquid-to-hexatic phase transition depending on the tracer shape (Fig. 4). In the case of diamond and square tracers, the decoupling occurs but with different trends. The translational diffusion of diamond tracers is enhanced compared to their rotational diffusion, which is consistent with previous experiments [1,8]. Surprisingly, in the case of square tracers, the rotational diffusion is enhanced compared to the translational diffusion. Distorted-diamond tracers do not show significant decoupling between D_T and D_R over the same range of T .

In order to investigate the SE and DSE relations, we calculate the translational relaxation time (τ_T) by using the self part of the intermediate scattering function

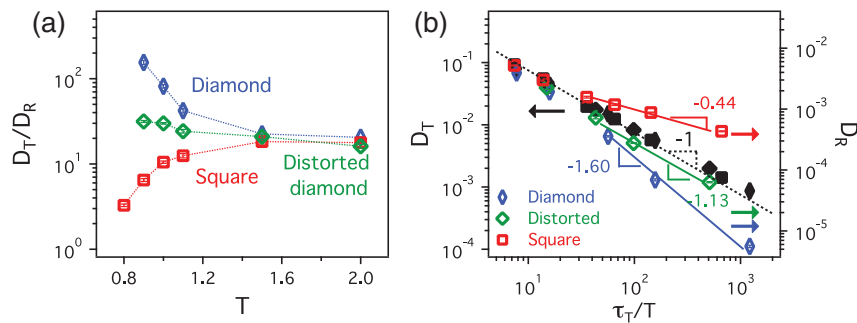


FIG. 4 (color). (a) D_T/D_R as a function of T for different shapes of tracers. (b) D_T (black open symbols and left axis) and D_R (colored filled symbols and right axis) as a function of τ_T/T . Solid lines are fits to simulation results. And a dashed line is a guide with an exponent of -1 .

$[F_s(k, t)]$ of each tracer. $F_s(k = 1.25\sigma^{-1}, t)$ follows the Kohlrausch-Williams-Watts (KWW) function, i.e., $F_s(k = 1.25\sigma^{-1}, t) \approx \exp[-(t/\tau_k)^{\beta_k}]$ [1]. We estimate τ_T by using $\tau_T \equiv \tau_k \Gamma(1/\beta_k)/\beta_k$, where Γ is the gamma function. Note that $2\pi/1.25$ corresponds to an approximate size of the tracers. The SE relation holds regardless of tracer shape with $D_T \sim (\tau_T/T)^{-1}$ but the DSE relation fails depending on the tracer shape [Fig. 4(b)]. Note that if we were to plot D_T as a function of τ_T instead of τ_T/T , the SE relation fails slightly with $D_T \sim \tau_T^{-1.15}$ even before the freezing transition, which was reported in Ref. [32]. Instead, D_R follows the fractional DSE relation, i.e., $D_R \sim (\tau_T/T)^\xi$ [5–7]. The values of ξ are -1.6 , -1.13 , and -0.44 for diamond, distorted-diamond, and square tracers, respectively. This indicates that the rotational diffusion of diamond tracers is suppressed more than expected by the DSE relation while the rotational diffusion of square tracers is enhanced more. In the meantime, the rotational diffusion of distorted-diamond tracers follows the DSE relation relatively well. Note that the trend of the DSE breakdown with tracer shape does not change significantly using D_R from the stretched $U_l(t)$ with $l \geq 2$ [30].

Such qualitative differences in the rotational diffusion of tracers may be attributed to whether the tracer shape is similar to the local structure of colloids and also to whether tracers may hop rotationally or not. Colloids around a diamond tracer are likely to form a hexagonal structure. On the other hand, colloids around a square tracer are less likely to form HBOO [Fig. 2(b)]. If a diamond tracer were to rotate, the structural similarity between the diamond tracer and colloids would be broken down transiently. In order for the diamond tracer to rotate, therefore, the colloids around the diamond tracer need to move in a collective fashion, which imposes a free energy barrier on the rotation of the diamond tracer and makes the diamond tracer undergo rotational hopping motions. As shown in Fig. 5, we calculate the rotational displacement distribution functions $G(\varphi_m, t) \equiv \langle \delta[\varphi_m - \varphi_m(t)] \rangle$, where $\varphi_m(t) \equiv [\varphi(t) - \varphi(0)] - 2m\pi$ for an integer m , ensuring that $0 \leq \varphi_m(t) < 2\pi$ [22]. There are several peaks in $G(\varphi_m, t)$ of diamond tracers, indicating that the diamond tracers prefer a particular set of angles, especially integer multiples of $\pi/3$.

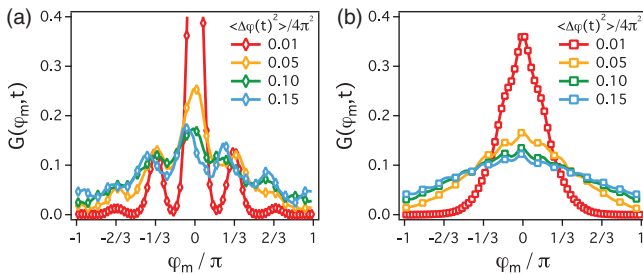


FIG. 5 (color). Rotational displacement distribution functions $[G(\varphi_m, t)]$ of (a) diamond and (b) square tracers.

This suggests that the diamond tracers should undergo rotational hopping motions by the angle of integer multiples of $\pi/3$.

Square and distorted-diamond tracers, on the other hand, do not hop rotationally as much as diamond tracers. This is because square and distorted-diamond tracers are not similar in structure to HBOO of colloids, which makes larger voids around the tracers [24]. The tracers undergo relatively normal Brownian rotational diffusion [Fig. 5(b)] [33].

D_T of tracers satisfies the SE relation because D_T is averaged over several dynamic domains. 2D colloids in hexatic phases consist of dynamic domains of different mobility. The approximate size of the dynamically correlated domain is estimated by calculating the dynamic susceptibility $\chi_4(t)$ [34]. The peak height of $\chi_4(t)$ reaches approximately 25 at $T = 0.9$, implying that the dynamic domain size is about 5 [30]. $\langle (\Delta r)^2(t) \rangle$ of tracers becomes linear with time t , only when $\langle (\Delta r)^2(t) \rangle \geq 100$ [30]. This indicates that the tracer diffusion enters a Fickian regime only after tracers should travel over several dynamic domains and that D_T should be averaged over several dynamic domains, thus D_T is obeying the SE relation.

In summary, we perform molecular dynamics simulations for tracers of three different shapes in 2D colloids. Around $T = 1$, 2D colloids undergo the liquid-to-hexatic phase transition and 2D colloids construct a quasi-long-range HBOO. We find that the translation and rotation of tracers decouple around $T = 1$, but with different trends depending on whether the tracer shape is similar to HBOO of colloids. In the case of diamond tracers, their shape is similar to HBOO, thus making the diamond tracers undergo rotational hopping motions and suppressing their rotational diffusion significantly. On the other hand, for square tracers, there are more voids around the square tracers because the square tracers are dissimilar to HBOO of colloids, which enhances the rotational diffusion more than expected by the DSE relation.

The translation-rotation decoupling phenomena reported so far were usually attributed to the DH of translation of tracers. On the other hand, we report a different case where the translation-rotation decoupling occurs due to the DH of the rotation of tracers and the breakdown of the DSE relation. The decoupling closely relates to the similarity between the tracer shape and the local media structure. Because tracers are employed as stand-ins to investigate the dynamics of host media, the effects of tracer shape in 2D colloids may indicate that the local structure should be critical to the DH. If the local structure of a certain region were to match with that of the surrounding (as for the diamond tracers), the particles in the domain would move only in collective motions, thus decreasing the mobility. This tracer shape effect would be also significant in network-forming liquids such as water, which forms hydrogen bond networks.

Our simulation results may call for more investigation on the connection between DH and the structural motif such as the LFSs [1–4]. In spite of the weak structural signature in 3D glass-forming liquids, many studies have been devoted to eliciting the structural origin of DH. For example, a LFS such as the icosahedron structure exists for the Wahnström mixture [4,35]. Recent studies showed that LFSs had different and broad lifetimes [4,35]. Some were short lived and broke down before the relaxation time of host glass formers. Others were, on the other hand, long-lived, thus persisting even after the relaxation time. Long-lived ones might have a tendency to be associated with DH. It would be an interesting topic of future studies investigating the dynamics of tracers of different shapes in 3D glass-forming liquids: tracers similar in structure to long-lived LFSs and tracers similar to short-lived ones.

This research was supported by Basic Science Research Program through the National Research Foundation of Korea (NRF) funded by the Ministry of Education, Science and Technology (NRF-2013R1A1A2009972). This research was also supported by the Advanced Research Center for Nuclear Excellence funded by MEST, Korea.

*bjsung@sogang.ac.kr

- [1] M. D. Ediger, *Annu. Rev. Phys. Chem.* **51**, 99 (2000).
- [2] M. D. Ediger and P. Harrowell, *J. Chem. Phys.* **137**, 080901 (2012).
- [3] L. Berthier and G. Biroli, *Rev. Mod. Phys.* **83**, 587 (2011).
- [4] C. P. Royall and S. R. Willians, *Phys. Rep.* **560**, 1 (2015).
- [5] T. G. Lombardo, P. G. Debenedetti, and F. H. Stillinger, *J. Chem. Phys.* **125**, 174507 (2006).
- [6] G. M. Mazza, N. Giovambattista, H. E. Stanley, and F. W. Starr, *Phys. Rev. E* **76**, 031203 (2007).
- [7] S.-H. Chong and W. Kob, *Phys. Rev. Lett.* **102**, 025702 (2009).
- [8] K. V. Edmond, M. T. Elsesser, G. L. Hunter, D. J. Pine, and E. R. Weeks, *Proc. Natl. Acad. Sci. U.S.A.* **109**, 17891 (2012).
- [9] D. B. Hall, A. Dhinojwala, and J. M. Torkelson, *Phys. Rev. Lett.* **79**, 103 (1997).
- [10] M. Kim, S. M. Anthony, S. C. Bae, and S. Granick, *J. Chem. Phys.* **135**, 054905 (2011).
- [11] R. Zondervan, F. Kulzer, G. C. G. Berkhou, and M. Orrit, *Proc. Natl. Acad. Sci. U.S.A.* **104**, 12628 (2007).
- [12] R. Zangi, S. A. Mackowiak, and L. J. Kaufman, *J. Chem. Phys.* **126**, 104501 (2007).
- [13] L. J. Kaufman, *Annu. Rev. Phys. Chem.* **64**, 177 (2013).
- [14] K. Paeng, H. Park, D. T. Hoang, and L. J. Kaufman, *Proc. Natl. Acad. Sci. U.S.A.* **112**, 4952 (2015).
- [15] C. K. Mishra and R. Ganapathy, *Phys. Rev. Lett.* **114**, 198302 (2015).
- [16] E. Flenner, H. Staley, and G. Szamel, *Phys. Rev. Lett.* **112**, 097801 (2014).
- [17] D. Chandler and J. P. Garrahan, *Annu. Rev. Phys. Chem.* **61**, 191 (2010).
- [18] J. Kim and B. J. Sung, *J. Phys. Condens. Matter* **27**, 235102 (2015).
- [19] M. M. Hurley and P. Harrowell, *Phys. Rev. E* **52**, 1694 (1995).
- [20] R. Zangi and S. A. Rice, *Phys. Rev. Lett.* **92**, 035502 (2004).
- [21] T. Kawasaki, T. Araki, and H. Tanaka, *Phys. Rev. Lett.* **99**, 215701 (2007).
- [22] K. Takae and A. Onuki, *Phys. Rev. E* **88**, 042317 (2013).
- [23] J. Kim, C. Kim, and B. J. Sung, *Phys. Rev. Lett.* **110**, 047801 (2013).
- [24] J. Kim and B. J. Sung, *J. Chem. Phys.* **141**, 014502 (2014).
- [25] S. Carmaker, C. Dasgupta, and S. Pastry, *Annu. Rev. Condens. Matter Phys.* **5**, 255 (2014).
- [26] E. Tamborini, C. P. Royall, and P. Cicuti, *J. Phys. Condens. Matter* **27**, 194124 (2015).
- [27] K. J. Strandburg, *Rev. Mod. Phys.* **60**, 161 (1988).
- [28] E. P. Bernard and W. Krauth, *Phys. Rev. Lett.* **107**, 155704 (2011).
- [29] <http://lammps.sandia.gov>.
- [30] See Supplemental Material at <http://link.aps.org/supplemental/10.1103/PhysRevLett.115.158302> for more details on a liquid-to-hexatic phase transition, void space around tracers, the dynamics of tracers, the effects of the presence and shape of tracers on 2D colloid dynamics, the estimates of dynamically correlated regions, tracer size effects on translation-rotation decoupling, the high-order rotational correlation and its effect on the decoupling, which includes Refs. [18, 21, 24, 27, 34].
- [31] P. Scheidler, W. Kob, and K. Binder, *Europhys. Lett.* **59**, 701 (2002).
- [32] S. Sengupta, S. Carmaker, C. Dasgupta, and S. Sastry, *J. Chem. Phys.* **138**, 12A548 (2013).
- [33] K. Mayoral, T. P. Kennair, X. Zhu, J. Milazzo, K. Ngo, M. M. Fryd, and T. G. Mason, *Phys. Rev. E* **84**, 051405 (2011).
- [34] N. Lačević, F. W. Starr, T. B. Schröder, and S. C. Glotzer, *J. Chem. Phys.* **119**, 7372 (2003).
- [35] A. Malins, J. Eggers, H. Tanaka, and C. P. Royall, *Faraday Discuss.* **167**, 405 (2013).